2020

An Automated Seepage Meter for Streams and Lakes

Douglas Kip Solomon

Eric Humphrey

Troy E. Gilmore

David P. Genereux

Vitaly A. Zlotnik

Water Resources Research

TECHNICAL REPORTS: METHODS
10.1029/2019WR026983

An Automated Seepage Meter for Streams and Lakes

D. Kip Solomon[1], Eric Humphrey[1], Troy E. Gilmore[2], David P. Genereux[3], and Vitaly Zlotnik[2]

[1]Department of Geology and Geophysics, University of Utah, Salt Lake City, UT, USA, [2]Biological Systems Engineering Department, University of Nebraska-Lincoln, Lincoln, NE, USA, [3]Department of Marine, Earth, and Atmospheric Sciences, North Carolina State University at Raleigh, Raleigh, NC, USA

Key Points:
- New seepage meter for streams and lakes has been developed
- Rapid seepage rate measurements can be made for several days
- The device can measure water levels to ±0.1 mm

Supporting Information:
- Supporting Information S1

Correspondence to:
D. K. Solomon,
kip.solomon@utah.edu

Citation:
Solomon, D. K., Humphrey, E., Gilmore, T. E., Genereux, D. P., & Zlotnik, V. (2020). An automated seepage meter for streams and lakes. *Water Resources Research*, *56*, e2019WR026983. https://doi.org/10.1029/2019WR026983

Received 23 DEC 2019
Accepted 29 MAR 2020
Accepted article online 4 APR 2020

Abstract We describe a new automatic seepage meter for use in soft bottom streams and lakes. The meter utilizes a thin-walled tube that is inserted into the streambed or lakebed. A hole in the side of the tube is fitted with an electric valve. Prior to the test, the valve is open and the water level inside the tube is the same as the water level outside the tube. The test starts with closure of the valve, and the water level inside the tube changes as it moves toward the equilibrium hydraulic head that exists at the bottom of the tube. The time rate of change of the water level immediately after the valve closes is a direct measure of the seepage rate (q). The meter utilizes a precision linear actuator and a conductance circuit to sense the water level to a precision of about ±0.1 mm. The meter can also provide an estimate of vertical hydraulic conductivity (K_v) if data are collected for a characteristic time. The detection limit for q depends on the vertical hydraulic head gradient. For K_v = 1 m/day, q of about 2 mm/day can be measured. Results from a laboratory sand tank show excellent agreement between measured and true q, and results from a field site are similar to values from calculations based on independent measurements of K_v and vertical head gradients. The meter can provide rapid (30 min) q measurements for both gaining and losing systems and complements other methods for quantifying surface water groundwater interactions.

1. Introduction

Quantifying groundwater seepage into or out of streams and lakes is important for both water balance and water quality studies. A variety of methods exist for quantifying seepage rate (specific discharge) (Kalbus et al., 2006) including seepage meters (e.g., Boyle, 1994; Cable et al., 2006; Lee, 1977; Libelo & MacIntyre, 1994; Rosenberry, 2008; Shaw & Prepas, 1990), a piezo-seep meter (Murdoch & Kelly, 2003), piezomanometers and associated field permeameters (Kennedy et al., 2007, 2009, 2010), stream tracer tests (Bencala et al., 1987; Gooseff & McGlynn, 2005; Harvey et al., 1996), and methods based on heat as a tracer (Conant, 2004; Constantz, 1998; Constantz & Stonestrom, 2003; Vogt et al., 2010).

Solder et al. (2016) utilized the idea of Bouwer (1961) and described a tube seepage meter for use in streams in which a thin-walled tube is inserted into a streambed. The tube seepage meter is different than prior versions of seepage meters in at least four aspects. (1) The "footprint" of the seepage tube is comparable to point-scale measurement devices (7.6 cm diameter or 45 cm^2). Most traditional seepage meters have larger footprints (Kalbus et al., 2006), for example, 2,550 cm^2 (Lee, 1977). (2) Tube seepage meters can make individual seepage measurements over relatively short periods of time (minutes) for both gaining and losing systems. Many seepage meter applications rely on the collection of a volume of water over hours or days to determine seepage rates (Kalbus et al., 2006). Exceptions are seepage devices equipped with tracer-based flow meters that use salt dilution (Gilmore et al., 2016; Solder, 2014), dye dilution or displacement (Koopmans & Berg, 2011; Sholkovitz et al., 2003), heat pulse sensing (Krupa et al., 1998; Taniguchi & Fukuo, 1993), ultrasonic meters (Paulsen et al., 2001), or electromagnetic meters (Rosenberry & Morin, 2004). (3) The tube seepage meter relies on direct measurement of hydraulic head inside the tube, which is different than the volumetric, tracer, ultrasonic, or electromagnetic flow meters. The piezo-seep meter is an exception (Kelly & Murdoch, 2003). (4) Most potential sources of error for classic seepage meters are minimized such as disturbance of stream head or groundwater velocity fields by the meter and potential friction losses within the meter and/or collection device (Belanger & Montgomery, 1992; Cherkauer & McBride, 1988; Corbett et al., 2003; Koopmans & Berg, 2011; Rosenberry & Menheer, 2006).

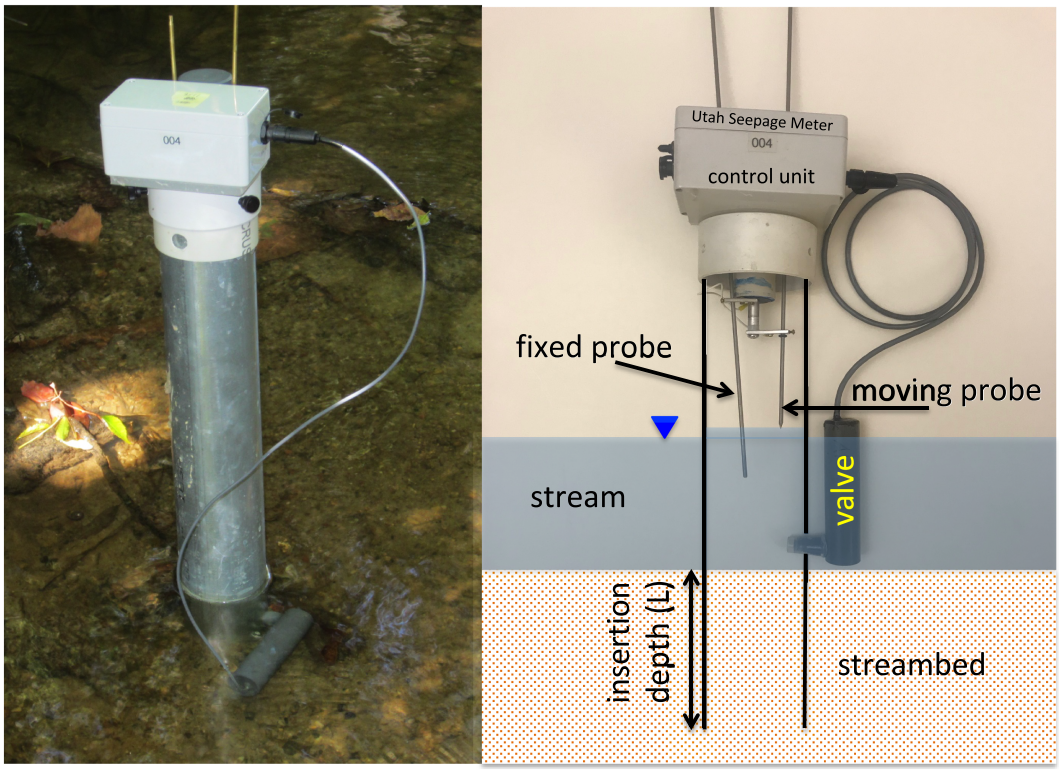

Figure 1. Photo and diagram of the seepage meter. The control unit (white box) sits on top of a sturdy thin-walled tube that is inserted into the streambed (typically 30 to 50 cm below the top of the streambed). A hole in the side of the tube (located just above the sediment-water interface) is fitted with a submersible electric valve (small gray cylinder outside the tube). At the beginning of the test, the valve is open so that the water level inside the tube is the same as outside the tube, in the stream. The valve then closes, and as the water level inside the tube changes (up for a gaining stream, down for a losing stream), it is measured by a moving probe that is automatically advanced by the linear actuator until the probe just contacts the water. Water levels and associated times are recorded by the control unit.

The objective of this paper is to describe the design and functioning of an automated tube seepage meter that is capable of measuring changes in water level as small as 0.1 mm which is a fundamental advance over the techniques described by Bouwer (1961) and Solder et al. (2016). The precision of the water level measurements allows measurements of seepage rate (specific discharge) as small as 2 mm/day under favorable conditions (see supporting information Figure S4). Typically, a single measurement can be made in less than 30 min. This allows assessment of temporal variability in q, which is difficult to measure with conventional seepage meters (Rosenberry et al., 2013). We also expand on the hydraulic theory of the meter to include a changing stream level and present preliminary results from the Sand Hills of Nebraska, USA.

2. Description

2.1. Meter

The seepage meter consists of a control unit (microprocessor), a moving probe driven by a linear actuator, and a valve (Figure 1). A stainless steel rod with a fine point on one end is attached to the linear actuator and used as a moving water level probe. A second stainless steel fixed probe is attached to electric ground on the meter and extends into the water inside the tube. To measure the water level, the linear actuator moves downward until the fine point of the moving probe touches the water surface, at which point a drop in resistance in the circuit between the two probes is detected by the control unit. The electronics in this unit are similar to a typical electric tape used for water level measurements and work well even in water of low electrical conductivity (down to about 5 μS/cm). Once the position of the linear actuator has been recorded, the moving probe is retracted until a rise in resistance is detected, when the fine tip leaves the water. The meter determines the water level based on the moving probe contacting the water surface rather than

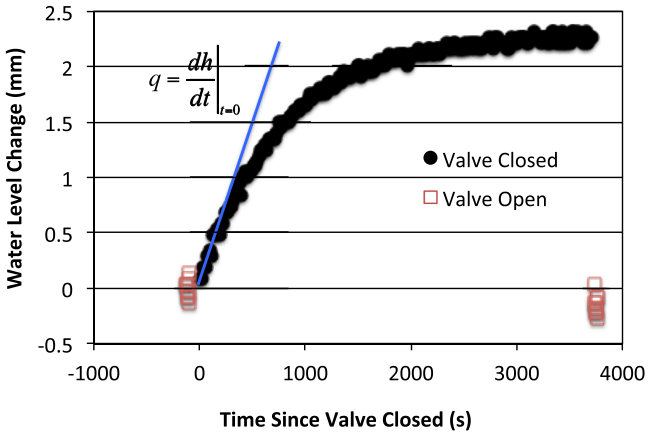

Figure 2. Example of seepage meter data from a test in the streambed of Hominy Swamp Creek in Wilson, NC. The slope (blue line) of the curve (black dots when valve is closed) at time = 0 gives the seepage rate (0.00248 mm/s = 0.214 m/day). Variability in the water level when the valve is open is due to turbulence in the stream stage.

being removed from the water. This results in more repeatable measurements by avoiding capillarity effects associated with water sticking to the probe upon retraction. The probe positions are adjustable to accommodate various stickup lengths of the thin-walled tubing.

At the beginning of a test, the control unit opens the electric valve so that the water level inside the tube is the same as in the stream or lake outside of the tube. The tube acts as a stilling well to dampen high-frequency variations in the outside water level. The water level is then measured 10 times and stored in memory. The control unit then closes the electric valve. The design of the valve is such that it does not cause a change in the water level upon closing. The meter then measures the water level inside the tube at regular intervals in time (typically every 30 s but programmable from 2 to 999 s) and stores the value in memory (Figure 2). After a programmable number of measurements (typically 50 to 200), the electric valve opens and the water level inside the tube returns to the stream or lake level. Finally, the water level measurements inside the tube are repeated 10 times, and all values in memory are written to an SD card in the control unit. The meter repeats the test until it is manually switched off or the battery charge is depleted. As explained below, the estimate of groundwater seepage rate is derived from the measurements of water level versus time collected while the valve is closed.

The position of the actuator (and hence the water level) is determined using a variable resistor, and the analog signal is digitized with a 10 bit (1,024 increments) analog to digital convertor. The actuator has a full-scale range of 50 mm (although 100 mm is possible), and thus, the meter's theoretical resolution for the water level is 50 μm/1,024 ≈ 0.05 mm.

Lithium ion polymer batteries that are rechargeable using any USB charger can power the meter for up to 3 days depending on the measurement frequency. Communication with the control unit for programming, downloading data, and real-time monitoring (if desired) is via a USB port using an Android app installed on a mobile device (phone, tablet, etc.) A micro SD card of up to 256 GB can store millions of tests (typical file size for 3 hr of measurements is less than 10 KB). The control unit is housed in a water-resistant (IP 64) case making it suitable for use in adverse weather but not prolonged submersion.

2.2. Seepage Rate Evaluation

The seepage rate evaluation is based on combining a water balance equation with Darcy's law (Todd, 1980). The equation for hydraulic head inside the tube as a function of time after the valve closure is (modified from Solder et al. (2016, equation (A.4)))

$$h = \frac{qL}{K_v}\left(1 - e^{-\lambda t}\right) + h_s \tag{1a}$$

$$\lambda = \frac{K_v D^2}{d^2 L} \tag{1b}$$

where h is the hydraulic head inside the tube after the valve closes (L), h_s is the hydraulic head of the stream water surrounding the seepage meter (L), q is the seepage rate (or vertical specific discharge) (L/T), and L is the depth of insertion of the tube into the streambed (see Figure 1) (L).

K_v is the vertical hydraulic conductivity of the streambed (L/T), D is the inside diameter of the lower part of the tube filled with sediment (L), d is the inside diameter of the upper part of the tube above the streambed (L), and t is the time since closing the valve (T). Equation 1a is functionally similar to equation (9) of Bouwer (1961) but explicitly shows the controls that K_v and L have on the head inside the seepage meter. The derivation of equations 1a and 1b assumes that the head at the base of tube does not change as upward seepage through the base is progressively slowed and diverted around the tube as the water level inside the tube rises (see the supporting information for a discussion of this assumption.)

The time derivative of 1a is as follows:

$$\frac{dh}{dt} = \frac{qD^2 e^{-\lambda t}}{d^2} \tag{2a}$$

which at time = 0 and with $D = d$ (i.e., a tube with uniform inside diameter) becomes

$$\left.\frac{dh}{dt}\right|_{t=0} = q \tag{2b}$$

Equation 2b indicates that the slope of a head versus time curve (e.g., Figure 2), evaluated at time = 0 (when the head inside the tube is equal to the stream head), is a direct measure of the seepage rate and is independent of the hydraulic conductivity of the streambed or lakebed. In principle, the estimate of seepage is the rate of the water level change inside the tube at $t = 0$ (the moment when the valve in the side hole of the tube is closed), assuming that the head inside the tube is equilibrated at h_s before the valve is closed. In practice, this estimate depends on the measurement uncertainty compared to the magnitude of the water level change, which can be very small. For example, a seepage rate of 0.01 m/day in a streambed with K_v = 10 m/day and a tube insertion depth of 0.5 m will have an equilibrium head inside the tube (with the valve closed) that is only 0.5 mm different than the starting head. In order to reliably determine the slope of the head versus time curve in this example, the error in water level measurements needs to be significantly smaller than 0.5 mm.

Equations 1a and 1b assume that the stream stage does not change over the period of the test, which is often not the case. The effect of a changing stream stage on the head inside the tube can be derived by applying the falling head equations to the tube in the absence of seepage, and then by superposition, adding this to 1a to obtain the combined effect. The head inside the tube due to a change in stream stage is

$$h = (h_o - h_e)e^{-\lambda t} + h_e \tag{3}$$

where h_o = head at the bottom of the tube before the stream stage changes, h_e = head at the bottom of the tube after the stream stage changes, λ is the same as given in 1b, and t is the time since the change in stream stage.

If we assume that the change in head at the base of the tube is the same as in the stream (i.e., we neglect the short lag time required for a pressure wave to propagate to the base of the tube as discussed in the supporting information), then

$$\Delta h_s = h_e - h_o \tag{4}$$

where Δh_s = the change in stream stage.

By defining Δh as the change in water level inside the tube due to a change in stream stage and by combining 3 and 4, we have

$$\Delta h = \Delta h_s\left(1 - e^{-\lambda t}\right) \tag{5}$$

Equation 5 describes the change in head inside the tube due to an incremental change in the stream stage. If the stream stage is considered to change in increments of Δh_s during each time increment Δt (see supporting information Figure S1), superposition can be applied and 5 written as follows:

$$\Delta h = \sum_{i=1}^{n} h_{si} - \sum_{i=1}^{n} h_{si} e^{-i\lambda\Delta t} \tag{6}$$

where n is the total number of incremental changes in stream stage over the period of a test ($n = t/\Delta t$), Δt = uniform time increment, and Δh_{si} = change in stream stage over each time increment i.

Finally, 6 can be combined (using superposition) with 1a to give the combined change in head inside the tube (Δh_c) due to both seepage and to a changing stream head as follows:

$$\Delta h_c = \frac{qL}{K_v}\left(1 - e^{-\lambda t}\right) + \sum_{i=1}^{n} h_{si} - \sum_{i=1}^{n} h_{si} e^{-i\lambda \Delta t} \tag{7}$$

Equation 7 was compared to numerical results from MODFLOW and its associated LAKE package (Merritt & Konikow, 2000) to simulate the water level dynamics inside the tube (similar to Burnette et al., 2016); the impermeable wall of the tube in the sediment was simulated using the Horizontal Flow Barrier package (Hsieh & Freckleton, 1993.) Three cases were simulated: The change in stream stage was equal to 0 (constant in time), +0.3 m/day (rising stream), and −0.1 m/day (declining stream). In all cases 7 and MODFLOW are in excellent agreement (supporting information Figure S2).

The response of the water level inside the tube to a changing stream level depends on the combination of seepage rate and the rate of stream stage change. The water level inside the tube can go up and then down, down then up, change linearly with time, and so forth (supporting information Figure S3); however, in all cases, the slope of the water level versus time curve at $t = 0$ gives the seepage rate. When the seepage rate is large such that errors in water level measurements are small compared to changes in the water level over time, only a small number of measurements are needed to accurately define the slope at time = 0 and 7 is not needed. However, when the seepage rate is small and errors in water level measurements become significant, measurements are needed over a longer period of time and accounting for changes in stream stage over this time as described by 7 becomes more important. Techniques for utilizing a longer time series of water level measurements to determine the seepage rate are described in the following section.

3. Data Analysis

The raw data from the seepage meter are the water level inside the tube as a function of time. Two general methods for calculating the seepage rate q from these data are presented here. The most straightforward method is to fit the data to a second-order polynomial of the form $h = At^2 + Bt + C$ (referred to as the polynomial method). The seepage is then given by (with $D = d$):

$$q = \left.\frac{\mathrm{d}h}{\mathrm{d}t}\right|_{t=0} = B \tag{8}$$

Furthermore, an estimate $\sigma_q$of the uncertainty in q can be made by assuming that it is equal to the uncertainty σ_B in the polynomial coefficient B: $\sigma_q \approx \sigma_B$. Thus, standard software such as the LINEST function in Excel can be used to estimate q and its associated uncertainty by least squares fitting of the polynomial to the data to find the coefficient B. An advantage of fitting the data to a polynomial as opposed to numerically differentiating the head versus time curve is that data beyond the first few measurements can be used thus greatly reducing the uncertainty in the slope at time = 0 that results from noisy head measurements. A disadvantage to the polynomial fit is that it is not functionally equivalent to 1a or 7, and thus, when used with a longer-time data set that approaches the equilibrium head in the seepage tube, it does not provide the best fit to the early time data which most define the seepage. As a practical matter, the polynomial fit can be limited to early time data, but the choice of early time is somewhat arbitrary as a polynomial cannot fit the data at times beyond approximately one characteristic time (t_c; see below), and t_c is not necessarily known a priori.

The second method for analyzing the seepage meter data is more rigorous. The method is to fit 7 to the head versus time data by adjusting q and K_v such that the sum of squares of the residuals (SSR) between model and observed water level data is minimized (referred to as the SSR method). The early time data from the seepage meter are mostly sensitive to q, whereas the later time data are more sensitive to K_v. In order to jointly determine both q and K_v, data need to be collected for about one characteristic time $t_c = \frac{d^2 L}{D^2 K}$ (t_c is the time to reach 63% of equilibrium). This is illustrated in Figure 3 that shows the relative standard deviation for both q and K_v as a function of the number of characteristic times over which data were collected. Data for Figure 3 were obtained by generating synthetic head versus time values using equations 1a and 1b and then randomly perturbing the head data using the NORM.INV (RAND(), mean, noise) function in Excel to introduce noise into the data. We then fit 7 to this data set using the Solver in Excel to minimize the SSR between the synthetic data set and 7 by adjusting q and K_v. The SolverAid (De Levie, 2004) was then used to estimate the

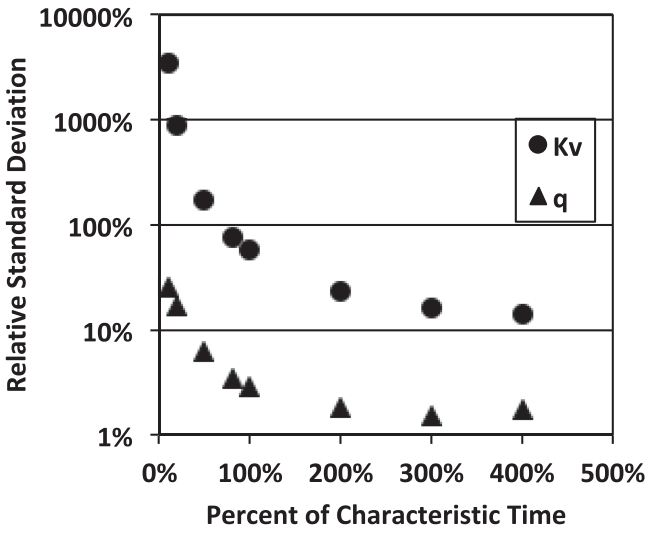

Figure 3. Relative standard deviation in deriving q and K_v by fitting 1a to synthetic data in which noise with a standard deviation of 0.1 mm was randomly added or subtracted from the head, as a function of the percent of the characteristic time over which data were collected. The uncertainty is especially large for K_v when the measurement period is less than one characteristic time.

uncertainty in the derived values for q and K_v. The SolverAid calculates standard deviations by considering the change in the calculated value with respect to changes in each of the input parameters (i.e., it calculates a sensitivity matrix). The uncertainty is especially large for K_v when the measurement period is less than one characteristic time (Figure 3).

When measurements are made for a time of t_c or longer, the uncertainty in q is a function of the vertical hydraulic gradient $\frac{q}{K_v}$ (supporting information Figure S4). The tube seepage meter is different than other seepage meters because the seepage rate measurement is based on measuring changes in water level, and the total change in water level is greatest when $\frac{q}{K_v}$ is large (either because q is large or K_v is small or some combination of these). Since the seepage rate is the derivative of the head with respect to time, evaluated at $t = 0$, and the uncertainty in time measurements is negligible, the uncertainty in q depends mostly on the uncertainty in measuring the head inside the tube. Large changes in head are more precisely measured than small changes. The relative standard deviation of q was computed using synthetically generated data as previously described using a water level measurement error of 0.1 mm. When $K_v = 1$ m/day, the seepage detection limit (defined by 100% error) is about 2 mm/day (supporting information Figure S4); the detection limit will be smaller for smaller values of K_v and larger for larger values of K_v.

It is clear from Figure 3 that measuring head changes for one characteristic time t_c or longer is important for the joint determination of q and K_v. However, this can lead to long measurement periods when K_v is small. For example, for a typical insertion depth of 0.5 m and K_v of 1 m/day, t_c is 0.5 days. While the meter is fully capable of measuring for this amount of time (and much longer), this leads to coarse temporal resolution if the objective is to examine changes in seepage through time and less replication of results even if seepage is temporally steady. In concept, it is also possible to build a seepage tube such that the diameter of the upper part of the tube (d in equations 1a) is smaller than the sediment-filled portion of the tube (D in equation 1a) (Solder et al., 2016) that will shorten t_c, but we have not yet tested this possibility. A practical alternative to measuring for one characteristic time is to combine an in situ falling head test (Chen, 2000; Genereux et al., 2008; Landon et al., 2001) with a short-term seepage meter measurement using the same tube. If only an estimate of seepage rate is desired, the polynomial fit to early time data can also be used (and is recommended), as previously discussed. We have generally found less than a 5% difference in the seepage rate computed using the SSR versus the polynomial analysis method.

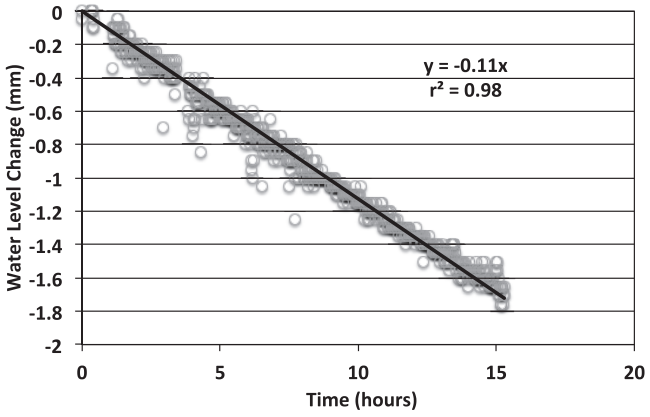

Figure 4. Water level change measured by a seepage meter installed in a 5 gallon bucket in the laboratory. The decline in water level is due only to evaporation. The standard deviation of the data after removal of the evaporation trend is 0.059 mm, which is similar to the resolution of the meter's analog to digital converter (0.050 mm). Less than 0.5% of the measurements were removed as outliers that generally coincided with ambient noise such as doors opening/closing and fans turning on/off.

4. Testing and Field Application

4.1. Laboratory Testing

Two different types of laboratory tests were conducted. We used the meter to measure water levels in a 19 L bucket in the laboratory that was left open to evaporation (Figure 4). The change in water level over a 15 hr interval was about 1.7 mm, corresponding to an evaporation rate of 2.7 mm/day. Measurements made over only the first 1.2 hr give an evaporation rate that is within 10% of the 15 hr mean and illustrate the ability of the meter to resolve very small temporal changes in water levels. The repeatability of the meter's water level measurements was assessed by removing the evaporation trend from the results shown in Figure 4. The resulting standard deviation ($n = 785$) was 0.059 mm, which is similar to the resolution of the meter's analog to digital converter.

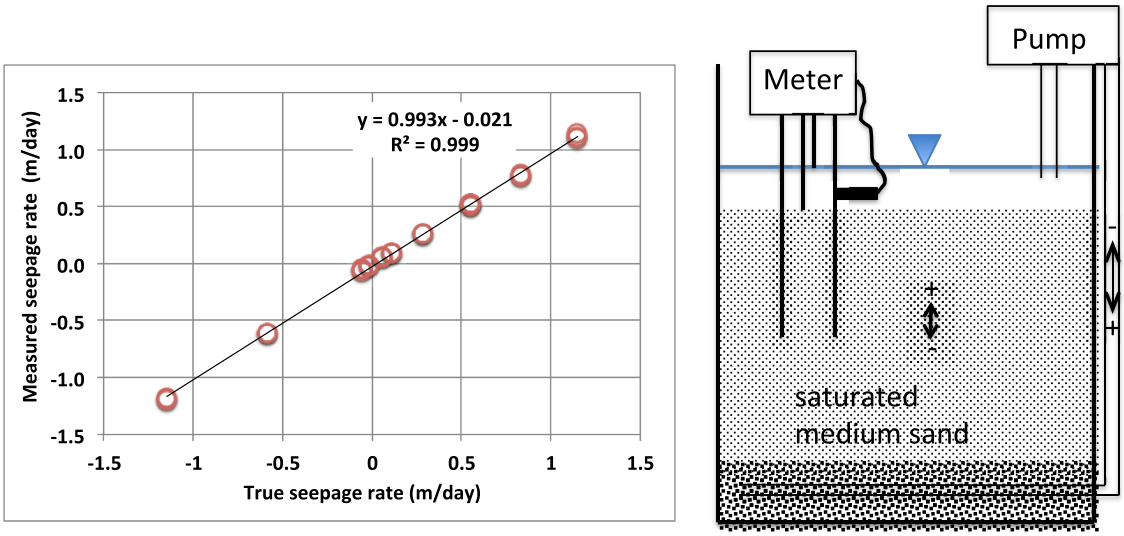

Figure 5. Comparison between seepage rate measured with the seepage meter and true seepage rate (pump rate divided by horizontal cross-sectional area of the tank) in a 250 L, 0.57 m diameter barrel filled with medium sand. Water was injected into the bottom of the barrel with a pump, flowed up through the sand in the barrel, and was recirculated to maintain a constant water level above the sand; the pump was also reversed to collect data under downward (negative) seepage.

The second type of laboratory tests consisted of measuring the seepage in a 0.57 m diameter by 0.85 m high sand tank (Figure 5). The tank was filled with medium sand, and a pump was used to circulate water between the top and bottom of the tank such that a constant vertical head gradient was maintained in the tank and constant vertical flow occurred through the sand. We compared the meter-determined seepage rate with that calculated by dividing the pumping rate by the cross-sectional area of the sand tank. The pump was run in one direction to create positive (upward) seepage and later simply reversed to produce negative seepage that is analogous to a losing stream. There is excellent agreement between the seepage values measured with the meter and computed as pump rate divided by tank cross-sectional area, with no apparent bias over a range of ±1.2 m/day.

4.2. Field Results

We simultaneously deployed nine seepage meters arranged in a 3 × 3 grid in the South Branch of the Middle Loup River located in the Sand Hills of Nebraska, USA. The grid spacing was approximately 1.5 m across the width of the stream and 3 m longitudinally along the stream. Individual measurements lasted for approximately 35 min starting at about 13:00 on 21 September 2018 and ending about 09:00 on 22 September 2018 (Figure 6). There was significant spatial variability in the seepage measurements with temporal averages ranging from +0.165 ± 0.02 to −0.001 ± 0.01 m/day. From 13:00 to 21:00 on 21 September 2018, the stream stage rose approximately 4 mm and then declined by about 8 mm from 21:00 on 21 September 2018 to 09:00 on 22 September 2018. Although this pattern is weakly followed by the seepage rate determined by some of the meters (e.g., Meters 007 and 001), the measurement uncertainty is generally as large or larger than changes through time. The mean value of all measurements (over time and space) is 0.054 ± 0.059 m/day. However, one of the meters (004) did not reproduce the same change in stream stage as the other eight meters and we suspect it was not functioning properly; the results from Meter 004 have been removed from the following discussion. The mean value excluding results of Meter 004 is 0.069 ± 0.059 m/day.

Adjacent to each of the nine seepage meters, a vertical hydraulic gradient measurement in the streambed and a falling head test for estimating the vertical K_v were performed in order to estimate seepage rate using the Darcy's equation. Vertical gradients were measured using a light-oil piezomanometer (Kennedy et al., 2007) installed near each seepage tube. Adding a small amount of water to each seepage tube while the electric valve was closed, and recording the subsequent drop in head, allowed the tube to function as a field permeameter for a falling head test (Chen, 2004; Genereux et al., 2008; Landon et al., 2001; Song et al., 2007). At each tube, K_v was estimated from the falling head data using the approach of Genereux

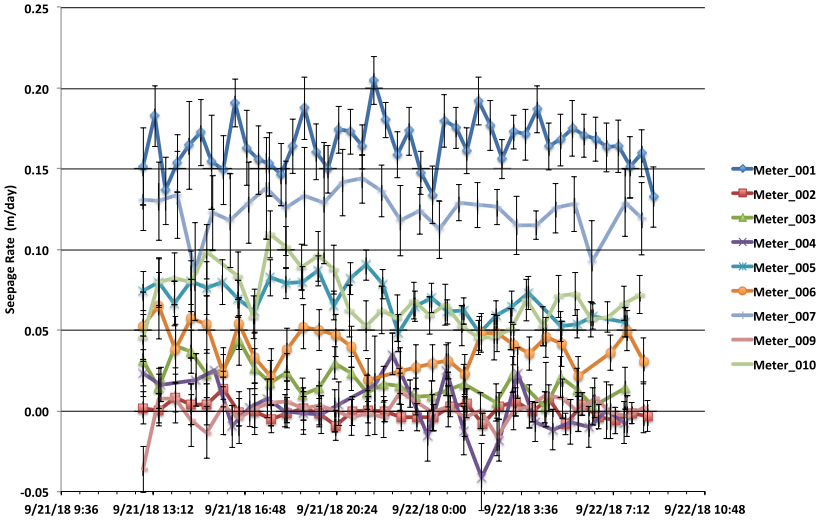

Figure 6. Seepage rate estimates from nine seepage meters deployed in the South Branch of the Middle Loup River in the Nebraska Sand Hills over a 20 hr period. The seepage meters were arranged in a 3 × 3 grid with a spacing of approximately 1.5 m across the stream and 3 m along the stream.

et al. (2008). While using the seepage meters in this manner was convenient, the limited vertical measurement range of the meters prevented us from increasing the head to the degree that is normally done for falling head tests (Chen, 2000; Genereux et al., 2008; Landon et al., 2001) and this resulted in relatively large uncertainty in K_v. The estimates of vertical hydraulic gradient and K_v were used in Darcy's law to calculate the seepage rate. The mean and standard deviation from Darcy's law are 0.036 ± 0.033 m/day (all points) or 0.041 ± 0.032 (1 point with 0 gradient removed; it is possible that the piezomanometer was not sealed into the sediments at this point).

Comparison of the seepage rates from the meters (q_{meter}) and from calculations with Darcy's law (q_{Darcy}) is complex (supporting information Figure S5), as has often been the case with similar comparisons in past work (Kennedy et al., 2010). For example, for linear regression of 53 paired values of q_{meter} and q_{Darcy}, Kennedy et al. (2010) found r^2 of 0.27; the r^2 value from our preliminary field measurements (supporting information Figure S5) is 0.39 (1 point removed). Kennedy et al. (2010) found that the difference between q_{meter} and q_{Darcy} was statistically significant at 53% of their streambed measurement points (28 of 53); in our work, it was 50% (four of eight). The ratio of mean seepage rates from the two methods (using all points), q_{meter}/q_{Darcy}, was 1.5 for our data, well within the range of values found in previous studies and closer to 1 than in some, for example, 6.7 (Lee & Cherry, 1979), 4.4 (Shaw et al., 1990), 0.7 (Kennedy et al., 2010), and 0.3 (Bokuniewicz et al., 2004).

Point-by-point comparison of paired q_{meter} and q_{Darcy} is challenging, with variability produced by such things as small-scale spatial variability in streambeds and lakebeds (q_{meter} and the head gradient and K_v needed for q_{Darcy} are generally measured in close proximity but not all three in the exact same location). Our field work with the automated tube seepage meter demonstrates that the meter functions as intended in the field; the case for the meter accuracy is made with the laboratory testing and not through the comparison of q_{meter} and q_{Darcy} in the field (supporting information Figure S5). Excellent agreement between the meter seepage rate and the true seepage rate was obtained in the lab (Figure 5), without the complexities associated with comparing q_{meter} and q_{Darcy} in the field.

5. Advantages and Limitations

The new tool for estimating water fluxes between groundwater and surface water has the following advantages:

1. The meter can provide a measure of both q and K_v and hence the vertical hydraulic gradient, q/K_v. It can measure both upward and downward seepage rates in the bed sediments, and the estimation of q is very simple requiring only that the head versus time data be fit to a second-order polynomial.
2. Seepage rate measurements can be made relatively quickly, (typically 30 min when only measurements of q are desired) allowing the assessment of temporal variability (see Rosenberry et al., 2013 for a discussion of temporal variability).
3. Determination of the direction of the vertical gradient (i.e., whether the stream is gaining or losing) requires only a few minutes.
4. The seepage meter can operate unattended for up to 3 days allowing temporal trends in q to be measured. The meter can also record changes in stream stage over time as small as about 0.1 mm/hr.
5. The seepage meter is capable of depth-specific measurements. The tube is typically installed to a depth of 0.3 to 0.5 m, but vertical profiles of q as a function of depth can be made by inserting the tube to greater depths in the bed sediments. In contrast, vertical profiling is not generally practical with larger traditional meters due to insertion difficulties.
6. Installing the small diameter tube is easier than installing a large traditional seepage meter, and measurements are averaged over a smaller area (the tube's cross section is about 45 cm^2). This can be an advantage or limitation depending on the goals of the project (i.e., delineating small-scale variations and features vs. large-scale integrated values.) Installing the small diameter tube is much easier than the installation of large traditional seepage meters, but measurements are integrated over a small area. In this regard, the seepage meter is well suited for mapping out streambed and lakebed variability that cannot be assessed with lower-resolution methods such as stream tracer tests.
7. The meter is relatively inexpensive. The components (linear actuator, electronics and connectors) can be purchased for the price of a typical inexpensive pressure transducer. However, the various plastic parts of the electric valve, actuator housing, and so forth require additional labor time and machining skill. These costs could be dramatically reduced if the parts are produced in volume.
8. Many of the problems associated with traditional seepage meters such as flow resistance within components of the meter (Murdoch & Kelly, 2003) and velocity head (Rosenberry, 2008) are eliminated with the tube seepage meter.

Some of the meter's limitations include the following:

1. The use of the seepage meter is limited to soft bottom and shallow streams and lakes (generally sandy beds with some silt and clay). We have installed tubes into gravelly streambeds, but the installation effects on natural seepage are currently unknown. In sandstone and other consolidated sediments modifications will be needed to provide an appropriate seal with the formation.
2. The seepage meter's tube must extend above to the surface of the lake or stream and can be interfered with by floating debris, recreational boats, vandalism, and so forth.
3. In low-K sediments, the measurement time can be long if both q and K_v are desired. This time may be reduced by making the inner diameter of the riser portion of the tube smaller than the sediment-filled portion, but we have not yet evaluated this possibility.
4. The range of measurable water level changes in this specific model is limited to 50 mm. When this range is exceeded, the meter does not function.
5. The 1-D (vertical) flow field assumed when deriving equations 1a and 1b becomes increasingly 3-D at the base of the tube with time as flow is diverted around the tube. Our sand box experiments and our 3-D numerical simulations indicate that this effect is negligible for a 7.6 cm ID seepage tube described in this paper; this is especially true shortly after the valve closes. However, the 3-D flow effects should be more significant for larger tube IDs and longer times, and these should be considered before scaling our results to larger tubes and/or longer times.

6. Summary

We have designed, tested, and applied a new seepage meter in soft bottom streams. The device consist of a thin-walled tube that is inserted into the streambed, and a linear actuator, which is capable of measuring water levels inside the tube with precision $\pm$0.1 mm. A hole in the side of the tube is fitted with an electric valve. Prior to the start of a test, the valve is open and the water level inside the tube is the same as the stream/lake. When the valve closes, the water level inside the tube rises in a gaining stream (or falls in a

losing stream) and is recorded as a function of time. The slope of the water level versus time curve just after the valve closure is a direct measure of groundwater seepage rate (q). The water level inside the tube exponentially approaches the hydraulic head at the base of the tube. The characteristic time (t_c) required to reach 63% of this head is $t_c = \frac{d^2 L}{D^2 K}$. If water level measurements are made for t_c or longer, it is possible to estimate both seepage rate q and K_v.

When the stream stage changes during a seepage test, the head in the streambed changes quickly, but the water level inside the tube is lagged because water must flow through the sediments inside the tube. We have incorporated the effects of a changing stream stage into the equation describing the water level response inside the seepage tube and tested it numerically. In all cases, the slope of the water level versus time curve at $t = 0$ gives the seepage rate, but the subsequent response of the water level is not always intuitive and requires additional analyses.

The uncertainty in q and K_v was investigated using representative examples; it depends on duration of data collection compared to t_c and the magnitude of the vertical hydraulic gradient (q/K_v). For $q/K_v = 0.01$ and measurements that last for t_c, our analysis suggests that the uncertainty in q and K_v will be less than 19% and 60%, respectively. For $q/K_v \geq 0.1$, the uncertainty in q is less than 2% when measurements last for t_c or longer.

Field testing of the meter in the Sand Hills of Nebraska demonstrates the meter's ability to evaluate temporal changes in seepage and spatial variations. The mean seepage rate obtained from eight measurements distributed over an area of 18 m^2 was 0.069 $\pm$ 0.059 m/day compared to 0.041 $\pm$ 0.032 m/day computed using Darcy's law. Differences may be due in part to spatial variability as it was not possible to make head gradient measurements at the exact location of the seepage meter.

The meter is an effective tool for studying the surface water-groundwater interactions at a small scale. It is relatively inexpensive to build and can detect seepage as low as 2 mm/day under favorable conditions and can typically provide useful measurements in less than an hour. The combination of low cost, practical accuracy, and rapid measurements opens the possibility to collect large data sets on water and mass fluxes across the surface water-groundwater interface.

Acknowledgments
The authors declare no conflict of interest. Data used for generating the figures in this manuscript can be found in the supporting information and associated data files and are archived online (https://doi.org/10.4211/hs.0646196da11d450a9d95c42c6568a25b). The field evaluation portion of this study was funded by the National Science Foundation Grant EAR-1744721. We thank Don Rosenberry, Larry Murdoch, and Joerg Lewandowski for excellent and helpful reviews of the manuscript. We thank Wil Mace for lab and field assistance developing the meter.

References

Belanger, T. V., & Montgomery, M. T. (1992). Seepage meter errors. *Limnology and Oceanography*, *37*(8), 1787–1795.

Bencala, K. E., McKnight, D. M., & Zellweger, G. W. (1987). Evaluation of natural tracers in an acidic and metal-rich stream. *Water Resources Research*, *23*(5), 827–836.

Bokuniewicz, H., Pollock, M., Blum, J., & Wilson, R. (2004). Submarine ground water discharge and salt penetration across the sea floor. *Groundwater*, *42*(7), 983–989.

Bouwer, H. (1961). Variable head technique for seepage meters. *Journal of the Irrigation and Drainage Division*, *87*(1), 31–44.

Boyle, D. R. (1994). Design of a seepage meter for measuring groundwater fluxes in the nonlittoral zones of lakes—Evaluation in a boreal forest lake. *Limnology and Oceanography*, *39*(3), 670–681.

Burnette, M. C., Genereux, D. P., & Birgand, F. (2016). In-situ falling-head test for hydraulic conductivity: Evaluation in layered sediments of an analysis derived for homogenous sediments. *Journal of Hydrology*, *539*, 319–329.

Cable, J. E., Martin, J. B., & Jaeger, J. (2006). Exonerating Bernoulli? On evaluating the physical and biological processes affecting marine seepage meter measurements. *Limnology and Oceanography: Methods*, *4*(6), 172–183.

Chen, X. (2000). Measurement of streambed hydraulic conductivity and its anisotropy. *Environmental Geology*, *39*(12), 1317–1324.

Chen, X. (2004). Streambed hydraulic conductivity for rivers in south-central Nebraska 1. *Journal of the American Water Resources Association*, *40*(3), 561–573.

Cherkauer, D. A., & McBride, J. M. (1988). A remotely operated seepage meter for use in large lakes and rivers. *Groundwater*, *26*(2), 165–171.

Conant, B. Jr. (2004). Delineating and quantifying ground water discharge zones using streambed temperatures. *Groundwater*, *42*(2), 243–257.

Constantz, J. (1998). Interaction between stream temperature, streamflow, and groundwater exchanges in alpine streams. *Water Resources Research*, *34*(7), 1609–1615.

Constantz, J., & Stonestrom, D. A. (2003). Heat as a tracer of water movement near streams. US Geological Survey Circular, (1260), 1–96.

Corbett, D. R., Cable, J. E., Shinn, E. A., Reich, C. D., & Hickey, T. D. (2003). Seepage meters and advective transport in coastal environments: Comments on" seepage meters and Bernoulli's revenge" by EA Shinn, CD Reich, and TD Hickey. 2002." Estuaries" 25: 126-132. *Estuaries*, *26*(5), 1383–1387.

De Levie, R. (2004). *Advanced excel for scientific data analysis*. USA: Oxford University Press.

Genereux, D. P., Leahy, S., Mitasova, H., Kennedy, C. D., & Corbett, D. R. (2008). Spatial and temporal variability of streambed hydraulic conductivity in West Bear Creek, North Carolina, USA. *Journal of Hydrology*, *358*(3–4), 332–353.

Gilmore, T. E., Genereux, D. P., Solomon, D. K., & Solder, J. E. (2016). Groundwater transit time distribution and mean from streambed sampling in an agricultural coastal plain watershed, North Carolina, USA. *Water Resources Research*, *52*(3), 2025–2044.

Gooseff, M. N., & McGlynn, B. L. (2005). A stream tracer technique employing ionic tracers and specific conductance data applied to the Maimai catchment, New Zealand. *Hydrological Processes: An International Journal*, *19*(13), 2491–2506.
Harvey, J. W., Wagner, B. J., & Bencala, K. E. (1996). Evaluating the reliability of the stream tracer approach to characterize stream-subsurface water exchange. *Water Resources Research*, *32*(8), 2441–2451.
Hsieh, P. A., & Freckleton, J. R. (1993). *Documentation of a computer program to simulate horizontal-flow barriers using the US Geological Survey's modular three-dimensional finite-difference ground-water flow model* (Vol. 92, No. 477). US Geological Survey.
Kalbus, E., Reinstorf, F., & Schirmer, M. (2006). Measuring methods for groundwater? Surface water interactions: A review. *Hydrology and Earth System Sciences Discussions*, *10*(6), 873–887.
Kelly, S. E., & Murdoch, L. C. (2003). Measuring the hydraulic conductivity of shallow submerged sediments. *Ground Water*, *41*(4), 431–439. https://doi.org/10.1111/j.1745-6584.2003.tb02377.x
Kennedy, C. D., Genereux, D. P., Corbett, D. R., & Mitasova, H. (2007). Design of a light-oil piezomanometer for measurement of hydraulic head differences and collection of groundwater samples. *Water Resources Research*, *43*, W09501. https://doi.org/10.1029/2007WR005904
Kennedy, C. D., Genereux, D. P., Corbett, D. R., & Mitasova, H. (2009). Spatial and temporal dynamics of coupled groundwater and nitrogen fluxes through a streambed in an agricultural watershed. *Water Resources Research*, *45*, W09401. https://doi.org/10.1029/2008WR007397
Kennedy, C. D., Murdoch, L. C., Genereux, D. P., Corbett, D. R., Stone, K., Pham, P., & Mitasova, H. (2010). Comparison of Darcian flux calculations and seepage meter measurements in a sandy streambed in North Carolina, United States. *Water Resources Research*, *46*, W09501. https://doi.org/10.1029/2009WR008342
Koopmans, D., & Berg, P. (2011). An alternative to traditional seepage meters: Dye displacement. *Water Resources Research*, *47*, W09506. https://doi.org/10.1029/2010WR009113
Krupa, S. L., Belanger, T. V., Heck, H. H., Brock, J. T., & Jones, B. J. (1998). Krupaseep—The next generation seepage meter. *Journal of Coastal Research*, *26*, 210–213.
Landon, M. K., Rus, D. L., & Harvey, F. E. (2001). Comparison of instream methods for measuring hydraulic conductivity in sandy streambeds. *Groundwater*, *39*(6), 870–885.
Lee, D. R. (1977). A device for measuring seepage flux in lakes and estuaries 1. *Limnology and Oceanography*, *22*(1), 140–147.
Lee, D. R., & Cherry, J. A. (1979). A field exercise on groundwater flow using seepage meters and mini-piezometers. *Journal of Geological Education*, *27*(1), 6–10.
Libelo, E. L., & MacIntyre, W. G. (1994). Effects of surface-water movement on seepage-meter measurements of flow through the sediment-water interface. *Applied Hydrogeology*, *2*(4), 49–54.
Merritt, M. L., & Konikow, L. F. (2000). *Documentation of a computer program to simulate lake-aquifer interaction using the MODFLOW ground-water flow model and the MOC3D solute-transport model* (No. 4167). US Department of the Interior, US Geological Survey.
Murdoch, L. C., & Kelly, S. E. (2003). Factors affecting the performance of conventional seepage meters. *Water Resources Research*, *39*, 1163. https://doi.org/10.1029/2002WR001347
Neuman, S. P. (1974). Effect of partial penetration on flow in unconfined aquifers considering delayed gravity response. *Water Resources Research*, *10*(2), 303–312.
Paulsen, R. J., Smith, C. F., O'Rourke, D., & Wong, T. F. (2001). Development and evaluation of an ultrasonic ground water seepage meter. *Groundwater*, *39*(6), 904–911.
Rosenberry, D. O. (2008). A seepage meter designed for use in flowing water. *Journal of Hydrology*, *359*(1–2), 118–130.
Rosenberry, D. O., & Menheer, M. A. (2006). A system for calibrating seepage meters used to measure flow between ground water and surface water.
Rosenberry, D. O., & Morin, R. H. (2004). Use of an electromagnetic seepage meter to investigate temporal variability in lake seepage. *Groundwater*, *42*(1), 68–77.
Rosenberry, D. O., Sheibley, R. W., Cox, S. E., Simonds, F. W., & Naftz, D. L. (2013). Temporal variability of exchange between groundwater and surface water based on high-frequency direct measurements of seepage at the sediment-water interface. *Water Resources Research*, *49*(5), 2975–2986. https://doi.org/10.1002/wrcr.20198
Shaw, R. D., & Prepas, E. E. (1990). Groundwater-lake interactions: I. Accuracy of seepage meter estimates of lake seepage. *Journal of Hydrology*, *119*(1–4), 105–120.
Shaw, R. D., Shaw, J. F. H., Fricker, H., & Prepas, E. E. (1990). An integrated approach to quantify groundwater transport of phosphorus to Narrow Lake, Alberta. *Limnology and Oceanography*, *35*(4), 870–886.
Sholkovitz, E., Herbold, C., & Charette, M. (2003). An automated dye-dilution based seepage meter for the time-series measurement of submarine groundwater discharge. *Limnology and Oceanography: Methods*, *1*(1), 16–28.
Solder, J. E. (2014). Quantifying groundwater-surface water exchange: Development and testing of Shelby tubes and seepage blankets as discharge measurement and sample collection devices. Masters thesis, University of Utah, Salt Lake City, Utah. http://content.lib.utah.edu/cdm/singleitem/collection/etd3id/3170/rec/1662 (accessed March 26, 2015).
Solder, J. E., Gilmore, T. E., Genereux, D. P., & Solomon, D. K. (2016). A tube seepage meter for in situ measurement of seepage rate and groundwater sampling. *Groundwater*, *54*(4), 588–595.
Song, J., Chen, X., Cheng, C., Summerside, S., & Wen, F. (2007). Effects of hyporheic processes on streambed vertical hydraulic conductivity in three rivers of Nebraska. *Geophysical Research Letters*, *34*, L07409. https://doi.org/10.1029/2007GL029254
Taniguchi, M., & Fukuo, Y. (1993). Continuous measurements of ground-water seepage using an automatic seepage meter. *Groundwater*, *31*(4), 675–679.
Todd, D. K. (1980). *Groundwater hydrology*, (2nd ed., 535 pp.). New York: Wiley. ISBN 047108641.
Vogt, T., Schneider, P., Hahn-Woernle, L., & Cirpka, O. A. (2010). Estimation of seepage rates in a losing stream by means of fiber-optic high-resolution vertical temperature profiling. *Journal of Hydrology*, *380*(1–2), 154–164.

Water Resources Research

Supporting Information for

An Automated Seepage Meter for Streams and Lakes

D. Kip Solomon[1], Eric Humphrey[1], Troy E. Gilmore[2], David P. Genereux[3], and Vitaly Zlotnik[2]

[1]University of Utah.

[2]University of Nebraska, Lincoln.

[3]North Carolina State University.

Contents of this file

Additional Supporting Information (Files uploaded separately)

"SeepageExampleFig2.csv"
"ChangeStreamStageFigS2csv"
"LabEvapTestFig4.csv"
"LabTestingFig5.csv"
"SummaryFieldSeepageFig6.csv"

Introduction

This document expands on the operational theory of the seepage meter and includes data that were used to generate the figures. Small data sets are in tables, whereas larger data sets are in attached files.

Text S1.

The file "SeepageExampleFig2.csv" contains data from the seepage meter and is presented as an example. The file consists of time and delta head values when the valve was closed and open. This is a comma separated values (CSV) file type.

Text S2.

Equation S1 assumes that the stream/lake stage does not change over the period of the test. As this is often not the case, especially when used in a stream, we investigated the effect of a changing stream stage on the estimation of seepage rate with the meter. When the stream/lake stage changes, the head at the bottom of the tube will also change, but this change will be lagged by the time required for transmitting a pressure change to the bottom of the tube. According to analyses by Neuman (1974), the time scale of the hydraulic head response of the aquifer to the head perturbations is controlled by the aquifer compressibility, hydraulic conductivity, and distance:

$$t^* = \frac{S_s L^2}{K_v} \quad (S1)$$

where:

S_s = the specific storage of the porous medium (the streambed, in the context of this discussion) [L^{-1}];

L = distance in the porous medium between where a head variation is imposed and where it is observed [L];

K_v = vertical hydraulic conductivity [L/T].

While the response time of the hydraulic head in the streambed/lakebed (from a changing stream/lake stage) at the bottom of the seepage tube is given by (3), the response of the water level inside the tube is given by (1a), which results from applying Darcy's Law for flow through the porous media inside the tube. The characteristic time (for a uniform

tube ID) associated with (1a) is $t_c = \frac{L}{K_v}$. This is the time to reach 63% of equilibration. The ratio of t_c to t^* $\left(\frac{t_c}{t^*} = \frac{1}{S_s L}\right)$ is on the order of 1000 to 10,000 for typical values of S_s and L. In other words, the time scale over which the water level inside the tube responds to a changing head in the streambed/lakebed (when the valve in the side hole of the tube is closed) is up to 10,000 times slower than the time scale of the head change in the sediments outside the tube. Thus, in our derivation of (6) we assume that a change in the stream/lake stage results in an instantaneous change in the head at the base of the tube (in the sediments). This assumption is then used to derive (7) that approximates the change in water level inside the tube as a result of a changing stream/lake stage combined with the change in water level due to seepage.

Equation (7) assumes that the head at the base of tube does not change as upward seepage is progressively diverted around the tube as the water level inside the tube rises. We tested this 1D assumption by solving the 3D groundwater flow equation ($\nabla^2 h = \frac{S_s}{K}\frac{\partial h}{\partial t}$ where h is hydraulic head, S_s is specific storage, K is hydraulic conductivity, and t is time) with a time-dependent specified-head boundary condition at the sediment-water interface outside of the seepage tube, and a head-dependent boundary condition inside the tube. The head-dependent boundary condition couples a water budget inside the tube with Darcy's law for flow through the sediments inside the tube. The 3D groundwater flow equation with the head-dependent boundary condition was solved using MODFLOW with its associated LAKE package (Merritt and Konikow, 2000). We used a domain that was 1 m by 1 m horizontally by 2 m vertically with 50 rows, 50 columns and 20 layers. The boundary conditions on the side of this domain were set to no flow

and a specified flux equal to the desired seepage rate was used on the bottom. The hydraulic conductivity was homogeneous and isotropic with a value of 1 m/d and S_s was set to 0.0001 m^{-1}. See Burnette et al. (2016) for details on numerically simulating the head inside a tube using MODFLOW. Figure S2 shows the MODFLOW results compared to (7). In all cases MODLFOW predicts a slightly higher head than (7), and this may be due to flow near the base of seepage tube becoming increasingly 3D with time as the head inside the tube rises (gaining stream or lake) and as natural seepage is diverted around the tube. The deviation between (7) and MODFLOW increases with time. However, for the geometry of the tube we simulated (cross-sectional area of 16 cm^2) the 3D effects appear to be small (less than about 5% after 1 day) and are essentially non-existent in the early-time data that are used to calculate the seepage rate. We compared the 16 cm^2 results with those from a tube with 4 times larger cross-sectional area. The calculated seepage rates (using the polynomial method) agree to better than 0.1%, but the water level in the larger tube was 2.6% higher after 1 day. These results indicate that the 3D effects increase with increasing diameter of the seepage meter, and should be considered by anyone wishing to apply (7) to a larger seepage tube.

Text S2.
The file "ChangeStreamStageFigS2.csv" contains data from MODFLOW simulations of the seepage meter and from the analytical solution presented as Equation (7). The file consists of time and delta head values for 3 different changing stream stage rates. This is a comma separated values (CSV) file type.

Text S3.
The file "LabEvapTestFig4.csv" contains data from the seepage meter measuring evaporation in a open bucket in the laboratory. The file consists of time and delta head values. This is a comma separated values (CSV) file type.

Text S4.
The file "LabTestingFig5.csv" contains data from the seepage meter installed on a laboratory sand tank. The "true" seepage was measured as the pumping rate divided by

the area of the tank. The file contains seepage values, seepage uncertainty values, and true seepage values. This is a comma separated values (CSV) file type.

Text S5.
The file "SummaryFieldSeepageFig10.csv" contains data from 9 seepage meters deployed in the South Branch of the Middle Loup River in the Sand Hills, Nebraska over a 20 hour period. The file contains time values (as days since 1900) seepage values, and seepage uncertainty values. This is a comma separated values (CSV) file type.

Table S1

% uncertain Kv	% uncertain q	% of characteristic time
3369.6%	25.8%	10%
868.2%	17.0%	20%
170.8%	6.4%	50%
75.8%	3.5%	80%
57.4%	2.9%	100%
23.3%	1.9%	200%
16.3%	1.5%	300%
14.1%	1.8%	400%

Table S1. Relative standard deviation in deriving q and Kv by fitting (1a) to synthetic data in which noise with a standard deviation of 0.1 mm was randomly added or subtracted from the head, as a function of the percent of the characteristic time over which data were collected.

Table S2

q/k	% uncertain q
0.001	189.1%
0.002	66.1%
0.004	34.1%
0.01	18.2%
0.02	9.4%
0.04	4.6%
0.1	1.8%
0.2	0.9%

Table S2. Relative standard deviation in the seepage rate (q) versus the vertical hydraulic gradient (q/Kv) when measurements are made for one characteristic time (te).

Table S3.

qmeter (m/d)	± (m/d)	qdarcy (m/d)	"+" uncert (m/d)	"-" uncert (m/d)
0.133	0.019	0.052	0.008	0.008
-0.003	0.010	0.001	0.001	0.001
0.014	0.013	0.025	0.007	0.007
0.055	0.009	0.052	0.009	0.009
0.031	0.014	0.083	0.016	0.016
0.119	0.023	0.069	0.035	0.035
0.002	0.016	0.002	0.003	0.003
0.072	0.012	0.000	0.036	0.000

Table S3. Seepage rate measured with the seepage meter and computed from Darcy's law.

Figure S1

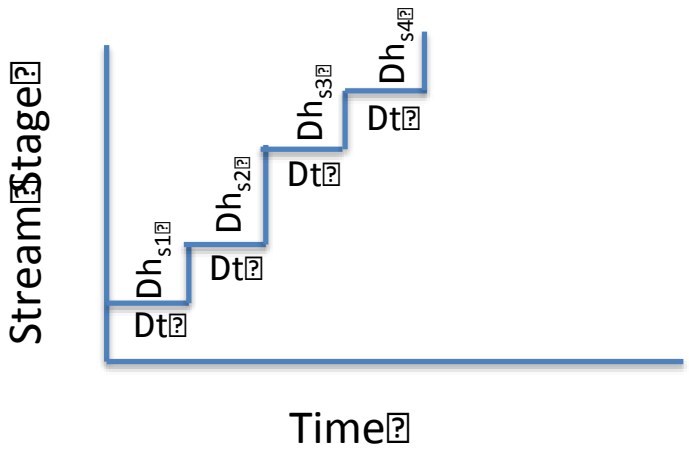

Figure S1 Discretization of a changing stream stage with time used in (6) and (7).

Figure S2

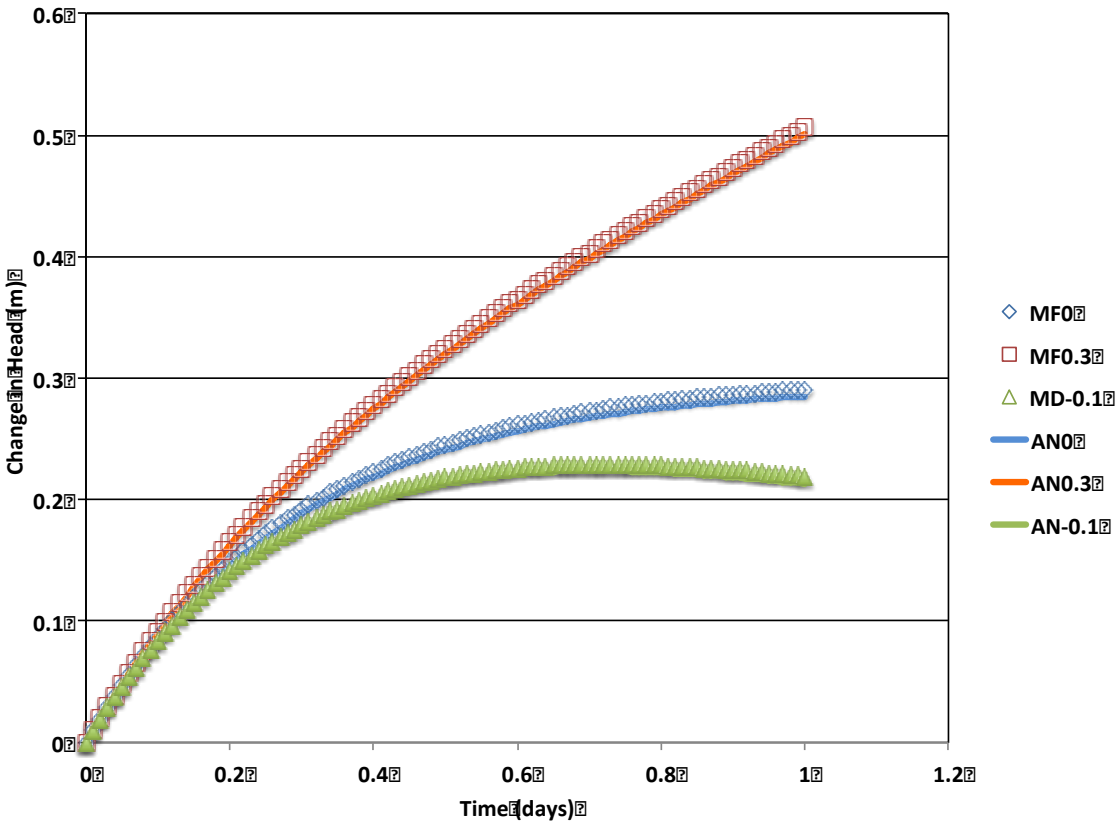

Figure S2 Comparison between values of water level changes in a seepage meter from analytical ((7), solid lines) and numerical (MODFLOW, open symbols) simulations of the seepage meter. The blue curves are for a stable stream stage, the orange curves are for a stream rise of 0.3 m/day, and the green curves are for a stream drop of -0.1 m/day. In all cases seepage was +1 m/day and K_v = 1 m/day. Note that the slope of all curves at time=0 gives the seepage rate and is independent of the changing stream stage.

Figure S3

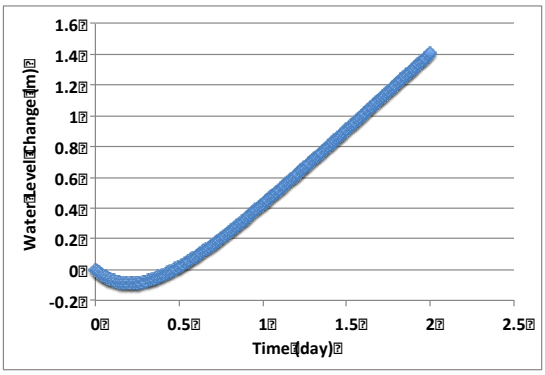

Seepage rate = 1 m/d (loss); K=1 m/d; change in stream stage = 1 m/d

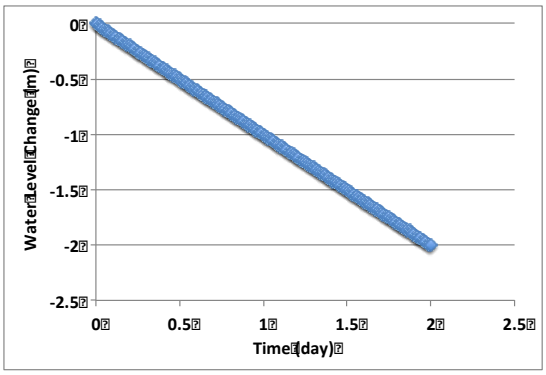

Seepage rate = -1 m/d (loss); K=1 m/d; change in stream stage = -1 m/d

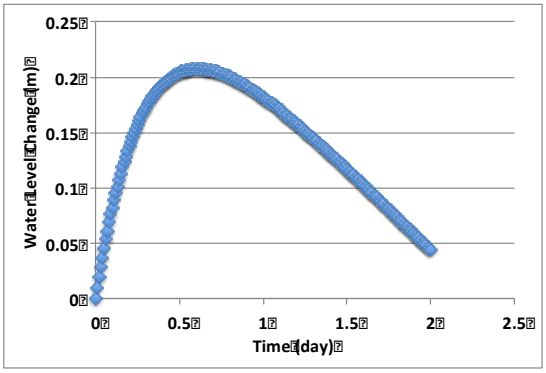

Seepage rate = 1 m/d; K=1 m/d; change in stream stage = -0.15 m/d

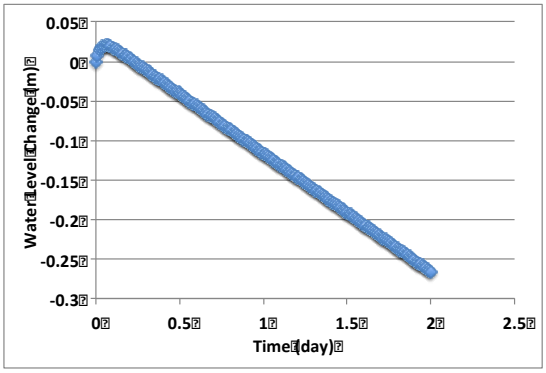

Seepage rate = 1 m/d; K=10 m/d; change in stream stage = -0.15 m/d

Figure S3 Examples of water level changes inside the seepage tube for various combinations of seepage rate and changing stream stage. The water level inside the tube can go up then down, down then up, change linearly with time, etc. In all cases, the slope of the curve at time = 0 gives the seepage rate.

Figure S4

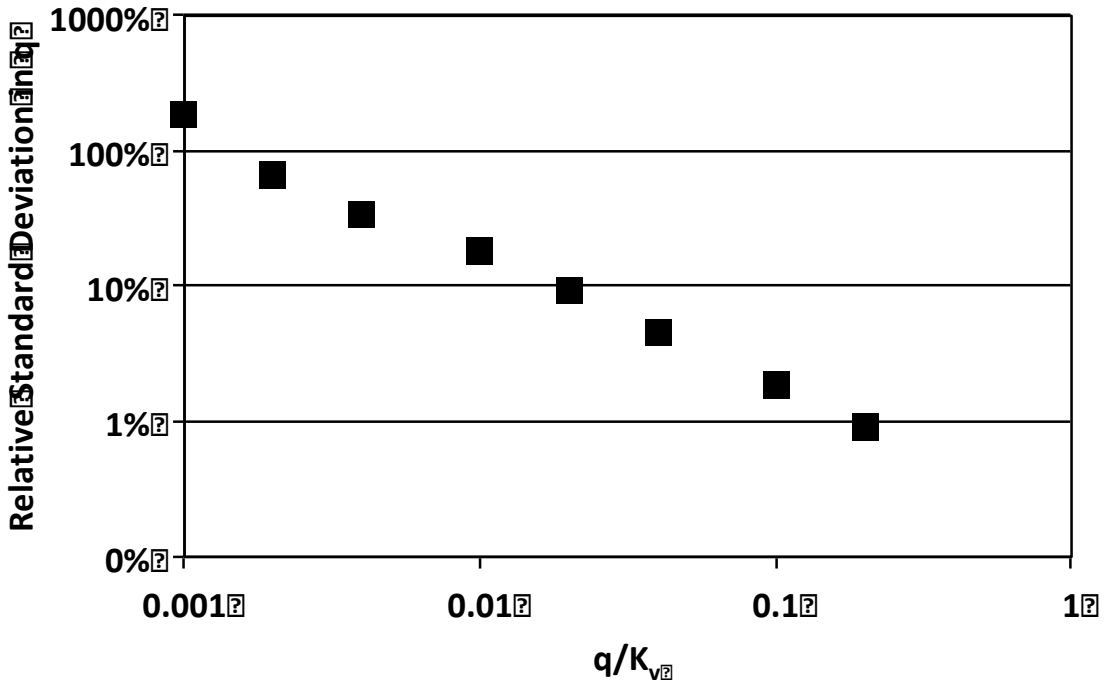

Figure S4 Relative standard deviation in the seepage rate (q) versus the vertical hydraulic gradient (q/K_v) when measurements are made for one characteristic time (t_c). For K_v = 1 m/day, the seepage detection limit (100% error) is about 2 mm/day. These results assumed a head measurement error of 0.1 mm.

Figure S5

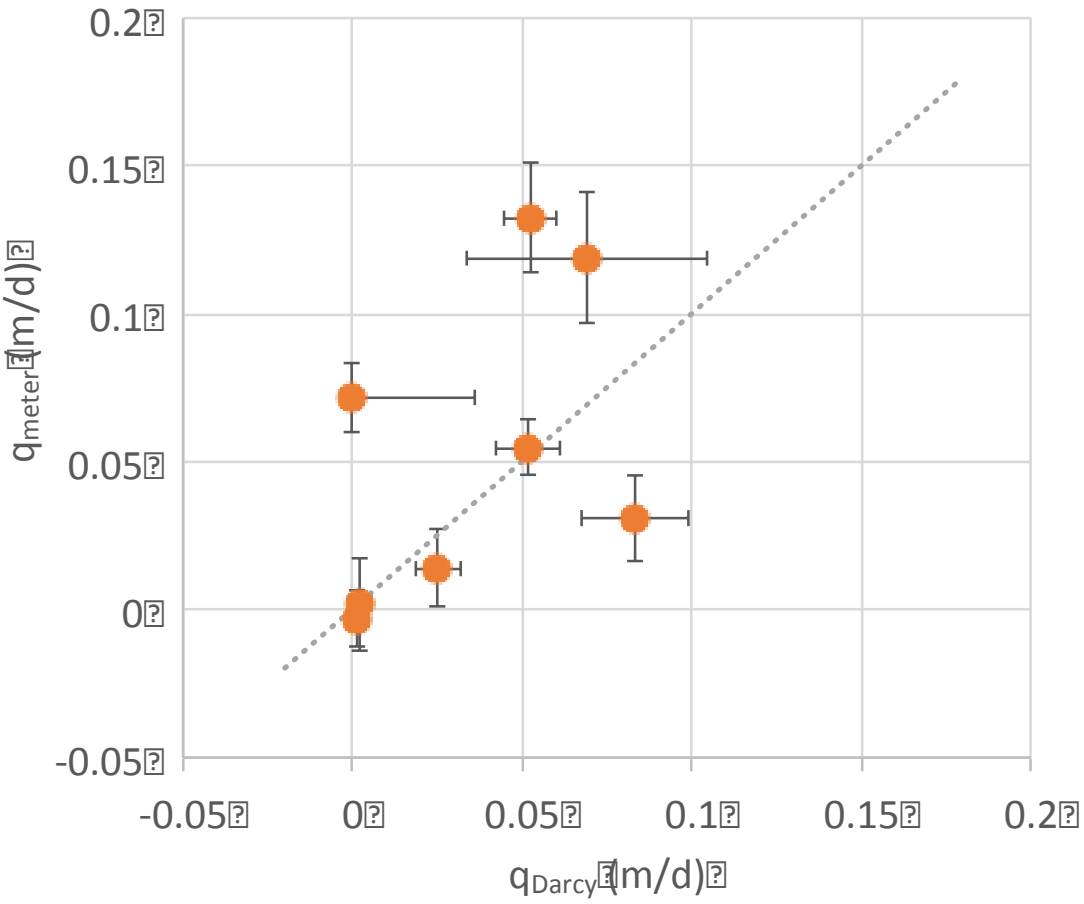

Figure S5. Comparison between seepage rate measured with the seepage meter and computed from Darcy's law.